Earth and Planetary Science Letters 452 (2016) 185–196

Contents lists available at ScienceDirect

Earth and Planetary Science Letters

www.elsevier.com/locate/epsl

Coseismic and postseismic displacements from the 1978 M_w 7.3 Tabas-e-Golshan earthquake in eastern Iran

Yu Zhou[a,*], Richard T. Walker[a], James Hollingsworth[b,c], Morteza Talebian[d], Xiaogang Song[e], Barry Parsons[a]

[a] COMET, Department of Earth Sciences, University of Oxford, Oxford OX1 3AN, UK
[b] Université Grenoble Alpes, ISTerre, 38058 Grenoble, France
[c] CNRS, ISTerre, UMR 5275, 38058 Grenoble, France
[d] Research Institute for Earth Sciences, Geological Survey of Iran, Azadi Square, Meraj Blvd, Tehran, Iran
[e] State Key Laboratory of Earthquake Dynamics, Institute of Geology, China Earthquake Administration, Beijing 100029, China

ARTICLE INFO

Article history:
Received 16 April 2016
Received in revised form 19 July 2016
Accepted 20 July 2016
Available online 16 August 2016
Editor: P. Shearer

Keywords:
1978 Tabas earthquake
historical optical imagery
afterslip
characteristic slip behaviour
continental tectonics
seismic hazard

ABSTRACT

We use optical image correlation of historical aerial photographs, and modern satellite images to investigate the 1978 M_w 7.3 Tabas-e-Golshan thrust earthquake in eastern Iran. Correlation of images between 1974 and 1991 reveals a near-surface shortening component of ∼2.9 m across the margin of the Tabas fold, which is a combination of coseismic and postseismic deformation. Correlation of images between 1991 and 2013 shows a further ∼0.3 m of postseismic shortening. Using six pre-earthquake aerial photographs acquired in 1956 and stereo SPOT-6 imagery from 2013, we also generate pre- and post-earthquake digital elevation models (DEMs) for one of the main fold segments. Differencing of the two DEMs reveals a height change of ∼4.7 m. Elastic dislocation modelling of the 1974–2013 displacement field requires 7 m slip on a 50° dipping fault, extending from a depth of 0.1 km to 6 km at its base (the majority of slip, ∼6.5 m, occurred prior to 1991). Our results, combined with previous InSAR observations, indicate time-decaying shallow postseismic afterslip. It is likely that most of the afterslip occurred prior to 1991. The slip appears to dissipate in the near surface, and is accommodated as a narrow band of flexural slip on bedding planes. Comparison of the fault slip model with terrace heights measured from the SPOT-6 DEM suggests that the Tabas fold system may exhibit characteristic slip behaviour. Such behaviour would require a magnitude M_w 7.3 earthquake every ∼3500 years, based on the previously estimated shortening rate of ∼1.0 mm/yr. This study highlights the usefulness of historical imagery in investigating past earthquakes, thus providing new information about historical faulting in continental regions.

1. Introduction

Measurements of surface deformation in earthquakes and by postseismic creep reveal how active folds and faults evolve over the seismic cycle (Burbank and Anderson, 2011; Copley, 2014; Dolan et al., 2003; Yu et al., 2003). They provide the most valuable source of data for the accurate description and understanding of continental tectonics, and for investigating present and future seismic hazard (Berberian, 1981; Hubbard and Shaw, 2009; Molnar and Lyon-Caen, 1989; Molnar et al., 1973; Tapponnier et al., 1990). Large continental earthquakes ($M_w \geq 7$) often occur on faults that were previously unmapped or poorly studied, due to the long recurrence times between events and their subtle geomorphological expression in the landscape (England and Jackson, 2011; Fialko et al., 2005; Funning et al., 2005; Jackson, 2001; Oskin et al., 2012; Zhang, 2013; Zhou et al., 2015a). Large blind thrust earthquakes, e.g. the 2015 Gorkha earthquake in Nepal (Elliott et al., 2016; Feng et al., 2015; Grandin et al., 2015; Wang and Fialko, 2015), have been uncommon in the era of modern satellite geodesy. Due to their hazardous nature, there is a strong need to re-examine older events to improve our understanding of the factors controlling the rupture of blind thrust faults.

The September 16, 1978 M_w 7.3 Tabas-e-Golshan earthquake in eastern Iran (hereafter referred to as the Tabas earthquake) is an example that occurred prior to the onset of interferometric synthetic aperture radar (InSAR) and Global Positioning System (GPS) monitoring, rupturing a series of previously unrecognised blind thrust faults. It is the only known large event in

* Corresponding author.
E-mail address: yu.zhou@earth.ox.ac.uk (Y. Zhou).

http://dx.doi.org/10.1016/j.epsl.2016.07.038

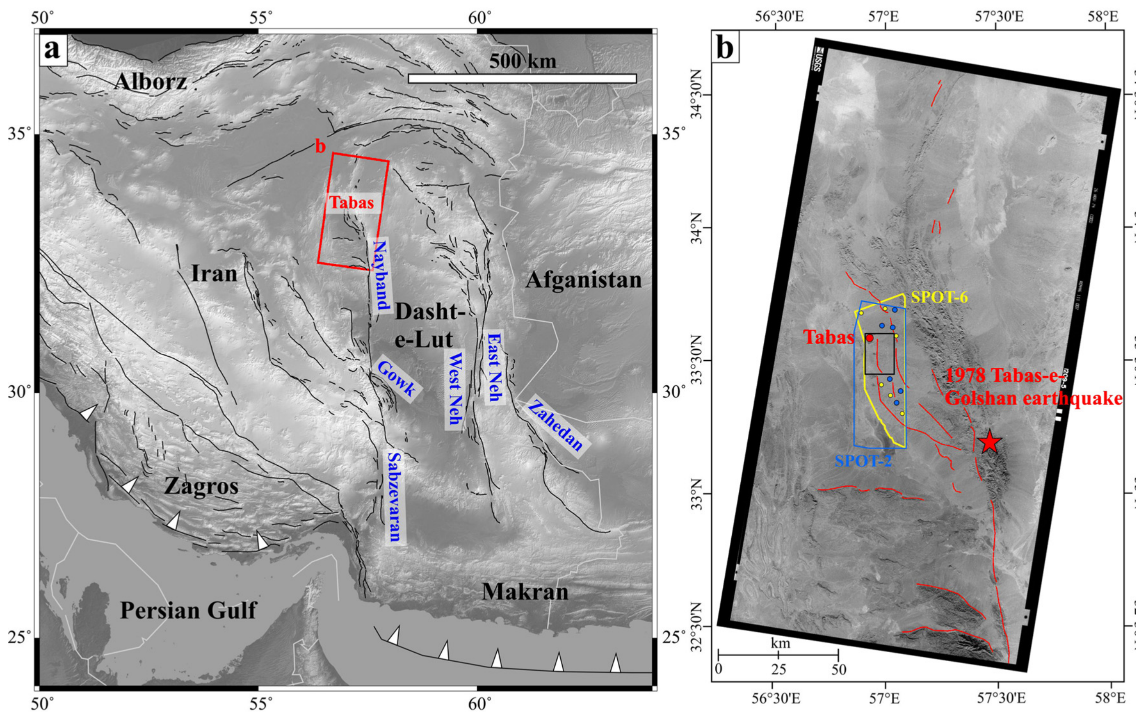

Fig. 1. (a) Active faults (black lines) in Iran, from Walker et al. (2003). Red box shows the coverage of the pre-earthquake KH-9 image. (b) KH-9 image around the Tabas region. Red star indicates the epicentre of the 16 September, 1978 Tabas-e-Golshan earthquake, from Walker et al. (2003). Red lines are active faults. Red dot indicates the location of Tabas. Yellow polygon shows SPOT-6 stereo image coverage (Fig. 2b). Yellow circles show the location of the GCPs used to co-register the KH-9 and SPOT-6 images. Blue polygon shows the SPOT-2 image coverage that we purchased for this study, with blue circles indicating the GCPs used to co-register the SPOT-2 and SPOT-6 images. Black box shows the area of Fig. 3a. (For interpretation of the references to colour in this figure legend, the reader is referred to the web version of this article.)

the epicentral area for at least the last 1,000 years, and completely demolished the oasis town of Tabas, killing ∼11,000 people, 85% of its population (Berberian, 1979; Berberian et al., 1979; Walker et al., 2003, 2013).

Berberian (1979) mapped 85 km of discontinuous surface ruptures 10 days after the 1978 earthquake. Much of the surface faulting took the form of small amounts of slip on multiple bedding planes, suggesting that much of the slip at depth failed to reach the surface and was instead accommodated as flexural-slip folding. The maximum coseismic vertical displacement localised on the main frontal thrust fault on the segment south of Tabas was measured to be ∼35 cm, but adjacent bedding slip totalled ∼150 cm (Berberian, 1979). Because most of the coseismic slip was concentrated at depth (Berberian, 1982; Walker et al., 2003), it is not possible to determine the pattern and magnitude of seismogenic slip and the sub-surface structure from mapping of discrete surface ruptures alone. No geodetic measurements of coseismic displacement exist, since GPS and InSAR monitoring were not available at the time of the 1978 Tabas earthquake. Nevertheless, Copley (2014) used InSAR to image shallow creep on the fold ∼6 km S–E of the town of Tabas (hereafter referred to as the Tabas fold) 30 years after the event.

The declassification of US Hexagon Keyhole-9 imagery (hereafter referred to as KH-9) allows us to investigate historical earthquakes back to the early 1970s (Burnett, 2012; Hollingsworth et al., 2012) as they provide a visual record of the landscape prior to the earthquake. In this study, we use sub-pixel optical image correlation to retrieve the coseismic and postseismic deformation fields. We first correlate KH-9 images acquired in 1974 with SPOT-2 satellite images acquired in 1991, and also modern high-resolution SPOT-6 data, to determine the horizontal displacements associated with the 1978 Tabas earthquake, from which we invert for the fault structure and earthquake slip. We also use six pre-earthquake aerial photographs acquired in 1956 and a post-earthquake SPOT-6 stereo data set acquired in 2013 to generate the pre- and post-earthquake topography respectively for one of the main fold segments (the same one as Copley, 2014). By differencing the pre- and post-earthquake topography, we measure the coseismic and postseismic height changes which allow us to better constrain the fault slip model. By reconciling our best-fit fault slip model with analysis of the long-term surface folding observed in the SPOT-6 topography, we constrain the 3D evolution of active thrust faulting in this region throughout the Late Quaternary.

2. Tectonic background of the 1978 Tabas earthquake

Iran is actively deforming in response to the collision of Arabia with Eurasia at a rate of ∼25 mm/yr at longitude 60° (Vernant et al., 2004a; Walker and Jackson, 2004). Regional deformation is characterised by distributed folding, reverse faulting, and strike-slip faulting (Berberian, 1981; Jackson et al., 1995; Walker and Jackson, 2004) (Fig. 1a). Studies based on plate models and GPS measurements indicate that up to half of the total Arabia–Eurasia shortening is taken up by north–south shortening in the Zagros mountains of southwestern Iran (∼10–15 mm/yr) (Hessami, 2002; Jackson et al., 1995; Tatar et al., 2002; Walpersdorf et al., 2006) with the Alborz accommodating a further 5 ± 2 mm/yr north–south shortening (Vernant et al., 2004b) and subduction of the South Caspian for another ∼5–10 mm/yr (Hollingsworth et al., 2008). The northward motion of central Iran relative to western Afghanistan results in ∼15 mm/yr north–south right-lateral shear (Mousavi et al., 2013; Walker and Jackson, 2004; Walpersdorf et al., 2014), accommodated across several right-lateral strike-slip faults bordering the Dasht-e-Lut Desert in eastern Iran. These include the East Neh (1.75–2.5 mm/yr from Meyer and Le Dortz, 2007), West Neh (1–5 mm/yr from Meyer and Le Dortz, 2007) and Zahedan faults in the east, and the Sabzevaran (∼6 mm/yr from Regard et al., 2006), Gowk (∼3.8–5.7 mm/yr from Fattahi et al., 2014; Walker et al., 2013) and Nayband (∼1.4 mm/yr from Walker et al., 2009 and ∼1.8 mm/yr from Foroutan et al., 2014) segments